In-Plane Permeability Characterization of Engineering Textiles Based On Radial Flow Experiments: A Benchmark Exercise

D. May[a,*], A. Aktas[b], S. G. Advani[c], A. Endruweit[d], E. Fauster[e], S. V. Lomov[f], A. Long[d], P. Mitschang[a], S. Abaimov[g], D. Abliz[h], I. Akhatov[g], T. D. Allen[i], D. C. Berg[h], S. Bickerton[i], M. Bodaghi[j], B. Caglar[k], H. Caglar[k], N. Correia[l], M. Danzi[m], J. Dittmann[n], P. Ermanni[m], A. George[o], V. Grishaev[g], M. A. Kabachi[m], K. Kind[p], M. D. Lagardère[q], M. Laspalas[r], P.-J. Liotier[s], C. H. Park[q], R. B. Pipes[t], M. Pucci[u], J. Raynal[v], E. S. Rodriguez[w], R. Schledjewski[e], R. Schubnel[v], N. Sharp[t], G. Sims[b], E. M. Sozer[k], R. Umer[x], B. Willenbacher[a], A. Yong[b], S. Zaremba[p], G. Ziegmann[h]

[a] Manufacturing Science, Institut für Verbundwerkstoffe GmbH, Germany
[b] Materials Division, National Physical Laboratory, United Kingdom
[c] Department of Mechanical Engineering, University of Delaware, USA
[d] Faculty of Engineering, University of Nottingham, United Kingdom
[e] Processing of Composites Group, Montanuniversität Leoben, Austria
[f] Department of Mechanical Engineering, Katholieke Universiteit Leuven, Belgium
[g] Skolkovo Institute of Science and Technology, Russia
[h] Institute of Polymer Materials and Polymer Technology, Technische Universität Clausthal, Germany
[i] Faculty of Engineering, University of Auckland, New Zealand
[j] Department of Mechanical Engineering, INEGI, Portugal
[k] Department of Mechanical Engineering, KOÇ University, Turkey
[l] Composite Materials and Structures Group, INEGI, Portugal
[m] Department of Mechanical and Process Engineering, ETH Zurich, Switzerland
[n] Institute of Aircraft Design, University of Stuttgart, Germany
[o] Faculty of Manufacturing Engineering Technology, Brigham Young University, USA
[p] Chair of Carbon Composites, Technische Universität München, Germany
[q] Department of Polymers and Composites Technology & Mechanical Engineering, IMT Lille Douai, France
[r] ITAINNOVA Instituto Tecnológico de Aragón, Spain
[s] Department Mechanics and Material Processing (MPE), École des Mines de Saint-Etienne, France
[t] Composites Manufacturing & Simulation Center, Purdue University, USA
[u] Ecole des Mines d'Alès, France
[v] Institut de Soudure Group, France
[w] Institute of research in Materials Science and Technology, Universidad Nacional de Mar del Plata, Argentina
[x] Department of Aerospace Engineering, Khalifa University, Abu Dhabi

*Corresponding author mail: david.may@ivw.uni-kl.de, phone: +49 631 31607 - 34

Abstract

Efficient process design for Liquid Composite Moulding requires knowledge of the permeability, which quantifies textile conductance for liquid flow. Yet, existing textile characterization methods have not yet been standardized, although good progress was made by two previous international benchmark exercises on in-plane permeability. The first one was without restrictions on the applied method and the second one focused on systems applying the linear unsaturated injection method. This paper presents the results of a third benchmark exercise on in-plane permeability measurement, based on systems applying the radial unsaturated injection method. In this benchmark study, 19 participants worldwide using 20 different systems participated. The participants were asked to measure the in-plane permeability of a non-crimp (NCF) and a woven fabric (WF) at three different fiber volume contents and at 5 repeats per fiber volume content. A commercially available silicone oil was used by the participants. A detailed characterization procedure was pre-defined, and each participant completed a complementary questionnaire on their measurement system characteristics (geometry, materials etc.), sensors (for pressure, temperature and flow front monitoring) and analysis methods. Excluding the outliers (2 of 20), the average coefficient of variation (cv) between the participant's results was 32% and 44% (NCF and WF), while the average cv for individual participants was 8% and 12%. This indicates systematic variations between the measurement systems. In this context, cavity deformation was identified as a major influence. If only data from the measurement systems with a cavity deformation < 2% (relative to the target value) are considered, the average cv reduces to 23% and 34% (NCF and WF). Further important sources of variation are fluid pressure / viscosity measurement, textile variations and data analysis. As a result, a strategy to minimise differences in in-plane permeability values from different systems will be drafted.

Keywords: Permeability, textiles, resin injection, resin flow, process monitoring

1. Introduction

Liquid Composite Molding (LCM) processes are employed for the manufacture of fiber reinforced polymer composites (FRPC), since they allow to efficiently manufacture components of different complexity and size at higher rates than autoclave processes. To obtain fast and complete saturation of the reinforcement with liquid resin in LCM, a suitable process design is required, which requires knowledge about material properties. The textile permeability is particularly important. It is defined by Darcy's law, which correlates the phase-averaged flow velocity, v, with the pressure gradient, ∇P, the dynamic fluid viscosity, μ, and the permeability, K, which quantifies the conductance of the porous media for liquid flow (Eq. 1).

$$\boldsymbol{v} = -\left(\frac{\boldsymbol{K}}{\mu}\right) \cdot \nabla P \qquad (1)$$

The permeability of fiber structures is generally direction-dependent and therefore described by a second-order tensor. Commonly, textile symmetry conditions are taken into account so that the tensor can be diagonalized, which leads to four remaining values describing flow in any direction within a fiber structure (assuming absence of coupling between in-plane and out-of-plane flow):

- Highest in-plane permeability (K_1), in-plane refers to the textile layer;
- Lowest in-plane permeability (K_2), oriented perpendicular to K_1;
- Orientation angle of K_1 (β), relative to the production direction of the material (0°);
- Out-of-plane permeability (K_3), oriented perpendicular to K_1 and K_2.

The present paper focuses on the characterization of the in-plane permeability (K_1, K_2 and β).

Despite the relevance of accurate permeability characterization for process efficiency, existing in-plane permeability characterization methods have not yet been standardized. There have been several smaller regional benchmarks studies [1-5]. Following them, in

2011, the results of the first truly international benchmark exercise on in-plane permeability measurement were published [6]. In this exercise, no specifications were made regarding the measurement method and the test parameters. This resulted in a scatter of the measured permeability values of more than one order of magnitude. A second international benchmark exercise with a predefined measurement procedure [7] followed. The participants were required to apply an unsaturated linear injection method. In unsaturated linear injection of a fluid into a dry reinforcement sample, one-dimensional flow develops. The resulting flow front movement can be tracked, and the permeability along the specimen axis can be derived using a 1D formulation of Eq. (1). This benchmark exercise showed - for this specific test method - that by defining minimum requirements for equipment, measurement procedure and analysis, satisfactory reproducibility of data obtained using different systems can be achieved [8]. In-plane permeability characterization based on radial flow experiments is an alternative approach, where the test fluid is injected through a central injection gate into a tool cavity containing the reinforcement sample. Advantages of this approach are that only one test is required for full textile characterization including K_1, K_2 and β and that the possible influence of race-tracking on test results is reduced. Hence, it was agreed at the 13th international conference on flow processes in composite materials (FPCM) in Kyoto (2016) to perform a third international benchmark exercise, focusing on unsaturated in-plane permeability characterization based on radial flow experiments. This benchmark exercise was organized by the Institute for Composite Materials (Kaiserslautern, Germany), and supported by the National Physical Laboratory (UK), the University of Nottingham, the University of Delaware (CCM), the Montanuniversität Leoben and KU Leuven as members of a steering committee. Table 1 lists the participants of the presented benchmark exercise.

2. Materials & Methods

2.1 Experimental set-up

2.1.1. Basic requirements

The presented benchmark focused on unsaturated in-plane permeability characterization based on radial flow. Taking into account the guidelines of the 2nd international benchmark on in-plane permeability characterization based on the linear flow method [7], basic requirements for the experimental set-up and the measurement procedure were specified:

- A stack of textile layers is compressed between two rigid mould surfaces at constant gap height (as illustrated in Figure 1).
- A test fluid is injected through a central circular hole (12 mm diameter, punched), resulting in a two-dimensional flow pattern (typically an ellipse).
- An unsaturated measurement principle is applied, i.e. flow front progression can be tracked.

2.1.2. Individual set-ups of the participants

Within the constraints of the stated basic requirements, a wide variety of designs of experimental set-ups was used by the participants. Table 2 gives an overview of the most important characteristics of the systems. Except for system #13, which is based on constant flow rate, all systems work with a constant injection pressure approach.

2.2 Materials

Two different reinforcement textiles were tested:

- A biaxial (±45°) glass fiber non-crimp fabric (NCF) from Saertex (X-E-444g/m²) with a nominal areal weight of 444 g/m² (217 g/m² in ±45° directions and additionally 1 g/m^2 and 2 g/m² in 0° and 90°, respectively, for stabilization) as well

as 6 g/m² polyester stitching yarn (76 dtex) with a warp pattern at a stitch length of 2.6 mm and a gauge length of 5 mm.

- A twill weave (2/2) glass fiber woven fabric (WF) from Hexcel (01102) with a nominal areal weight of 290 g/m² equally distributed in weft and warp direction. Nominal construction is 7 yarns/cm in weft and warp direction.

Both fabrics are nominally balanced. The actual construction of WF is somehow different in warp and weft direction: ends (warp) count is 7.13 yarns/cm, picks (weft) count is 7.00 yarns/cm. For both textiles, all participants in this study received material from the same batch, in order to minimise the influence of potential manufacturing variations on the benchmark results. Figure 2 shows surface images of both textiles.

The silicone oil XIAMETER® PMX-200 SILICONE FLUID 100CS supplied by Dow Corning was used as test fluid for permeability measurement. Its viscosity is approximately 100 mPa·s at room temperature. In order to minimize possible variations induced by the fluid viscosity, the silicone oil was procured batch-wise. For each of the ten batches used by different participants, the viscosity was centrally measured at TU Munich in a temperature range from 15 °C to 40 °C using an Anton Paar MCR 302 rheometer. This silicone oil was used by all participants except for participant #12, who used polymer solution in water as a test fluid, as the silicone oil caused problems with their sensors for flow front monitoring.

2.3 Test plan

The participants were asked to perform measurements on the non-crimp fabric (NCF) and the woven fabric (WF) as listed in Table 3. Although the number of layers can have an influence on measured permeability due to effects of nesting between layers and edge effects at the fabric-tool interface [17], all measurements were performed at a single cavity height but different number of layers to minimize the effort for spacer frame manufacturing. Also,

since the differences between the numbers of layers are small, and the minimum number of layers is eight, the influence of the number of layers on the permeability was regarded as negligible. Together with the number of layers and the nominal areal weight of the tested textiles, the defined cavity height defines the target fiber volume contents, shown in Table 3. Based on exploratory tests, injection pressures were specified in order to avoid possible effects of injection pressure on measured permeabilities. The pressure values were chosen to obtain meaningful test times which were assumed to be between one and five minutes. No vacuum was applied at the outlet during the tests.

Every test series comprised five tests with the same configuration (15 tests per textile).

2.4 Data Analysis

Analysis of raw data acquired in the tests, i.e. fitting of an ellipse to measured points on the flow front and calculation of permeability values based on the process conditions and the development of the flow ellipse geometry with time, was performed by each individual participant for their respective data. Table 4 sums up the analysis methods employed by the participants. It is to be noted that all methods used here (Chan/Hwang [18], Adams Rebenfeld [17, 19-21] and Weitzenboeck et al. [22, 23]) are based on different formulations of the same approach, transformation of an elliptical flow front shape to an equivalent isotropic co-ordinate system.

2.5 Sample preparation

For preparation of the test specimens, all participants were asked to follow these pre-defined steps:

In the first step, the individual fabric layers were cut out of the material at the required size and shape (determined by each participant’s injection tool geometry) and then stacked at

identical orientation according to Figure 3. The number of layers in each test specimen was defined by the test plan (Table 3).

In the second step, the inlet hole with a diameter of 12 mm (requirement) was punched into the stack. Punching of the complete stack was defined as requirement as cutting the hole may result in yarns being displaced. Also, if the hole is integrated into the individual layers, the following stacking process can lead to offset and therefore insufficient accuracy.

In the third step, each specimen was weighed for calculation of the actual fiber volume content.

2.6 Evaluation of cavity deformation

The participants were asked to evaluate experimentally the cavity deformation in their injection tool and the corresponding deviation from the target cavity height of 3.00 mm. For this purpose, blocks of plasticine, liquid metal filler (metal epoxy) or similar materials were placed in the tool cavity at five points according to the scheme shown in Figure 4, where P5 is located as close as possible to the inlet. The tool was closed, compressing the material blocks to a thickness corresponding to the cavity height. After opening of the tool, the thickness of the material blocks was measured to determine the cavity height. Two cases were considered: i) an empty tool, ii) a tool filled with the NCF at the highest tested fiber volume content (58 %). For the second test, holes were cut in the stack at the places where the plasticine was placed. From the five values per case, an average effective cavity height was calculated and compared to the target cavity height.

3. Results

Tables 5 and 6 list the main results of all participants. It is to be noted that participant #2 acquired permeability data using two different set-ups (see Table 2), while participants #7

and #17 provided two data sets, one as measured, and one with correction for deviations in cavity height.

Figures 5 and 6 summarise the measured permeability values for the NCF and the WF, respectively. Each figure contains two diagrams, showing the highest (K_1) and lowest (K_2) in-plane permeability value (logarithmic scale) as a function of the fiber volume content. In each diagram, the blue diamonds, the red squares and the green triangles show the results for the lowest ($V_{f,1}$), intermediate ($V_{f,2}$) and highest ($V_{f,3}$) target fiber volume content, respectively. Each data point represents the arithmetic average of the five repeat measurements conducted by each participant. The error bars show the standard deviation for permeability and fiber volume content. Deviations from the target fiber volume content are induced by areal weight variations, which were taken into account by weighing every specimen and calculating the individual fiber volume content for every test. In these figures, calculation of the fiber volume fraction is based on target values for the cavity height, not on the actually measured values.

In the diagrams, almost all data sets lie within a cluster at each nominal fiber volume content. Series #1 and #19 are exceptions for each data point, i.e. for both textiles, K_1 and K_2, and for each fiber volume content (data set #1 is incomplete, if they are not marked in the diagram then there was no data available). Also, the relative position of these two data sets to the cluster is always the same, indicating a systematic deviation. These data sets were excluded from further statistical analysis since they are obvious outliers. Several effects are suspected to contribute to the deviation, as will be discussed in the following sections. On the other hand, this means that 18 of the 20 data sets are included in the cluster and can be considered for statistical analysis.

Each cluster covers a range of about two percentage points of fiber volume content (e.g. 46% to 48%). While these variations in fiber volume fraction can have a strong effect on the

permeability, there is no correlation of permeability and fiber volume content within each cluster, indicating that other effects causing variation in permeability are dominant.

For the cluster range, the coefficient of variation (cv) of the permeability values measured at each single fiber volume content was calculated. The results listed in Table 7 show that the average for the cv was 32.2% and 43.9% for the NCF and the WF respectively. The target of the benchmarking efforts is to reach a point at which the variations between the results gained with different systems is no larger than the variation between the results gained on a single system. On average, the cv for individual data sets was 7.8% and 12.2% for the NCF and the WF respectively. Hence, there is further potential for improvement, which leads to the question which sources of variation can be identified based on the results. In the following sections, different potential sources are examined in detail.

In addition to K_1 and K_2, the orientation of the highest and lowest in-plane permeability relative to the fiber directions values was determined in the tests. Figure 7 shows the results for both textiles at each of the three nominal fiber volume contents. Each blue line in the graphics indicates the direction of K_1, averaged out of the five tests for each indivdual participant. The red dashed line shows the average of the data of all participants.

Both textiles show an average orientation where the highest permeability is approximately aligned with the fabric production direction. Yet, there is significant variation between the participants, especially for the NCF. A possible explanation might be given by the anisotropy of permeability, which is defined as the ratio of K_2 to K_1. The closer this ratio is to one, the more circular the flow front shape is formed. As the orientation angle is derived from the ellipse fitted to the flow front, a near-circular shape increases the influence of irregularities in the flow front shape. Table 8 lists the anisotropy for both textiles. It is close to 1 for the NCF, while the WF shows relatively high anisotropy – this presumably results from the deviations from the balanced fabric construction, mentioned in section 2.2, which

leads to the appearance of the gaps between the tows in production direction (see Figure 2). The anisotropy of NCF can be caused by the presence of stitching, oriented in the production direction. It is emphasized that the relative length of the half-axis corresponds to $\sqrt{K_1}/\sqrt{K_2}$, i.e. for the NCF the short half-axis is only about 12% shorter than the long half-axis.

In summary, the results show that for radial flow measurements the error in orientation angle determination increases with decreasing anisotropy. The variability is small when the anisotropy is high. This seems acceptable, since the relevance of the orientation angle decreases the more circular the flow front gets.

Both orientation angle and anisotropy did not show a clear dependence on the fiber volume content.

4. Discussion

4.1 Influence of cavity deformation

The data listed in Table 7 clearly shows that the variation between the results of the different institutions increases with increasing fiber volume content. This indicates an influence of the fiber volume content, which is presumably related to increasing cavity deformation with increasing fiber volume content as a result of increasing textile compression and also to increasing injection pressure. While comparably stiff systems remain closer to the target height of 3.00 mm, the less stiff ones show increasing cavity height, presumably related to tool deflection, which leads to increasing variation between the results.

To estimate the influence of deformation in detail, Figure 8 shows the results of the cavity height measurements. The figure contains a green, dashed line at 2 % deviation showing the originally proposed acceptable limit for deviation, which was defined based on the guideline for Benchmark II [7].

The results show that 10 out of 20 systems show a deviation greater 2% when the textile is compacted in the cavity. Relating this data to the materials used for the system (Table 2), one can see that of the seven full metal systems two showed deviation greater 2% while this was the case for eight out of thirteen systems which were fully or partially made of glass or PMMA. This indicates that neither usage of full metal system guarantees satisfying stiffness,nor usage of glass or PMMA necessarily leads to unsatisfying stiffness, although it tends to make systems more prone to deflection. Hence, it can be concluded that appropriate tool design is the key to minimising cavity height variations.

The influence of the deformation becomes clear when only the 10 systems with deviation from target cavity height smaller than 2% are considered for statistical analysis. In this case, the average for the cv reduces to 23% and 34% for the NCF and the WF respectivels. This gets close to the average cv found in Benchmark II which was approximately 20% for systems with deviation between actual and target cavity height smaller than 2. Yet, different textiles were measured in this benchmark, so it only makes sense to compare orders of magnitude of variation.

At this point, it is important to distinguish between parallel and non-parallel cavity height deviation, whereas the latter can be due to a pressure-induced deflection or a parallelism issue between top and bottom molds. It is practically impossible to correct the fiber volume content due to possible deflection, as the deflection is not uniformly distributed over the sample area and depends, among other factors, on the compaction behavior of the textile in dry and wet state as well as the fluid pressure. Both are not constant during the experiment, as the flow front propagates. Yet, if there is parallel deviation from the target, and this is measured, it can be accounted for when calculating the effective fiber volume content. Table 9 shows the normalized non-parallel deformation ω for all participants (Eq. 2). It is defined

as the ratio of σ_h, the standard deviation of the cavity height at the five measurement points (with textile in cavity), to θ_h, the arithmetic average of the five values.

$$\omega = \frac{\sigma_h}{\theta_h} \quad (2)$$

Some participants observed relatively large average deviations but only small non-parallel deformation, so that applying a correction to the fiber volume fraction was possible (#7 and #17 in Tables 5 and 6). Yet, as the corresponding values were only given for one test case, this was not investigated in detail.

It has to be emphasized that these observations and all other results in this paper represent the state of development given during the benchmarks.

4.2 Influence of fluid pressure measurement

The injection pressure to be used in the tests was pre-defined (Table 3) in order to minimize possible influences of pressure on permeability results. Among the 20 systems used in the benchmark, two provided a pressure sensor located directly at the proportional valve of the pressure vessel, eleven had a sensor somewhere in the feed line between oil reservoir and tool, and five had a tool-mounted sensor. The rest used the nominal pressure value to which the proportional valve is set for calculation. Two basic possibilities for an influence of fluid pressure on the calculated permeability are given.

Firstly, the injection pressure itself might influence the permeability: Darcy's law assumes a rigid porous media. However, textiles can deform under the fluid pressure. Hence, it could make a difference which injection pressure is applied during permeability measurement, especially as with the radial-flow approach the pressure is strongly localized at the beginning of the measurement. Pressure loss in the feed line between the pressure vessel and the tool can cause deviations of the actual injection pressure from the target pressure set at the vessel. Even if this is taken into account for permeability calculation by using sensor

data captured close to the injection point, this means the actual injection pressures among the participants varied. Yet, as the sensor values fairly accurately match the target values, this effect is estimated to be negligible for this benchmark. One of the 20 systems is based on a constant flow rate approach instead of constant injection pressure like the others. As the resulting data set was part of the cluster, no further statement is possible on the effect of this difference.

Secondly, pressure loss in the feed line between the sensor and the injection point can cause calculation errors. Within the benchmark, feeding line diameters and lengths from pressure sensor to injection point ranged from 4 mm to 12 mm and 50 mm to 5500 mm, respectively. At the given injection pressures, this can cause variation between the results. Further influence might be given by the fact that some participants use a pressure sensor value averaged over the complete test for permeability calculation and some use the single value of each time step.

All in all, since different influences contribute to variations, the benchmark results do not allow further statements. This would require tests with a focus on this influence.

4.3 Influence of fluid viscosity

Temperature-dependent viscosity is considered by all participants when calculating permeability via Darcy´s law. Yet, there may be several sources of variation.

Opposing the assumptions underlying the application of Darcy`s law, differences in viscosity could have secondary effects on the permeability, e.g. different deformation behavior of the preform or variations in wetting behavior. However, these influences are considered to be very small since the viscosity was in the range between 87 mPas and 113 mPa·s at temperatures between 17.3 °C and 27.4 °C, i.e. the temperature dependence is weak.

The viscosity for each single test is calculated using a viscosity-temperature function and the measured temperature. As can be seen in Table 2, participants measure the temperature at different locations: in the pressure vessel, the feed line, the tool or in the laboratory. This can lead to differences between the temperature measured and the actual temperature of the fluid within the tool. Also, temperature might vary during the test as not all participants have air-conditioning systems where the tests are performed. The data base does not allow a detailed statement about the influence of this effect.

Regional suppliers were selected for the silicone oil and the viscosity was centrally measured by TU Munich. The participants received the raw data of the measurements and individually fitted empirical functions to the viscosity- temperature data. At 23 °C, the measurement results of the batches showed an average variation of 1.7%. Yet, two participants measured the dynamic viscosity of the silicone oil with their own systems. The dynamic viscosity values at room temperature, derived from the different functions applied in the benchmark, show a cv of 3.8%. This indicates that additional uncertainty was induced by the diverse fitting functions.

Participant #1 received oil from a different batch than the other participants and measured the viscosity using their own equipment. Interestingly, the fitted function shows the highest values of all functions applied in the benchmark study. This could be an actual difference of this specific batch, but it could also indicate that there is a systematic difference between the measurements carried out by TU Munich and by this participant. While this is speculative, it highlights a very important issue: Variations between the viscosity measurements performed on different systems will directly add to variations between permeability data measured at different research sites.

Even though it was tried to exclude influences of the viscosity, it presumably has an effect that is not negligible. Therefore, efforts for standardization of permeability measurement need to involve aspects of fluid-induced variations.

4.4 Influence of fluid wetting behavior

Silicone oil as a substitute for resins is a commonly used test fluid in experimental studies of saturated and unsaturated permeability [8]. The choice of this type of fluid is based on its viscosity which is comparable to the one of liquid epoxy resins used for composite manufacturing. So far, capillary effects controlling wetting phenomena and potentially inducing void formation have been mostly neglected for those measurements. Silicone oil is a totally dispersive liquid (such as n-hexane) with a very low surface tension that makes it a totally wetting liquid. On the other hand, uncured liquid epoxy resin is a partially wetting fluid with a very different behaviour, due to its surface tension and components thereof [24]. Results of wicking tests with carbon fibers along the fiber direction, which have been conducted with silicone oil, therefore strongly differ from tests conducted with epoxy resin or water [25]. Hence, wicking of silicone oil into carbon reinforcements cannot be described by the common equations used for permeability estimation (Darcy or even Washburn equations). It is also impossible to consider a capillary pressure [25] for silicone oil. This could indicate that viscosity should not be the only parameter informing the choice of a non-reactive fluid as a substitute for liquid resin. Further studies should therefore focus on the identification or formulation of a physico-chemically reliable test liquid for permeability measurements.

4.5 Textile variations

Further variation between the participants' data might be induced by textile variations. Figure 9 shows the average areal weights measured for the test specimens by each participant. The error bars show the standard deviation. Although all material was from the same batch, there are some deviations between the participants, exceeding the variation for the single participants. However, the differences are still relatively small and they were considered in calculating the fiber volume content. But variations in areal weight also indicate variations in the textile structure, such as straightening of yarns which would affect the crimp of the WF. This would then also have an influence on permeability.

The cause for these variations may be related to the rewinding procedures in the context of the material distribution, to the individual layup and cutting procedures, or to the textile manufacturing process itself.

4.6 Influence of data analysis

Characterization of textile permeability basically comprises three steps: (1) Acquisition of relevant sensor data; (2) flow front modelling and allocation of pressure and viscosity values for each time step (eventually including time-averaging of pressure and viscosity values); and (3) computation of in-plane permeability data. The 20 systems compared in the benchmark differ in terms of type, number and location of sensors for temperature, pressure and especially flow front monitoring (see Table 2). Accordingly, step (1) and (2) necessarily differ. Table 4 shows that the algorithms used for step (3) are also different.

The variations induced by the differences in steps (1) and (2) depend on the flow front shape. For an ideally homogeneous porous media, resulting in a perfectly elliptical flow front, it does not matter if the ellipse is fitted to several thousand values (optical systems) or only three (minimum when center is fixed), assuming that the sensor data is reliable. Yet,

imperfections in the textile lead to local variations which can have a strong impact on measured permeability if they occur near a sensor. This impact increases with decreasing number of sensors. Inaccuracy of flow front detection also induces variation. The distance of the sensors to the inlet can have an influence, as the inlet is circular, while the algorithms applied in step (3) assume that it is of the same shape as the flow front. This causes an error that decreases with increasing distance of the flow front to the inlet. Hence, it can make a difference where the sensors are located. This, however, was not examined in detail because the superposition of different causes of variation does not allow isolating these effects.

Concerning step (2), two approaches exist for fitting an ellipse equation describing the flow front to sensor data. Either, the center of the fitted ellipse is forced to coincide with the injection point, or the center is allowed to float if this leads to a better fit. Both cases are illustrated in Figure 10.

The floating center approach may lead to a better fit. Yet, the algorithms used in step (3) are based on the assumption that flow spreads radially from the ellipse center and that the pressure has a maximum at this point. However, this is only true when the center is fixed to the injection point [4]. It is evident that using different strategies can lead to variations. 4 out of 20 have used the floating center method.

The algorithms used for step 3 are known to show some differences when applied to the same data [26]. Additional variation can be induced by the exact strategy with which the algorithm is applied to the data. Four strategies can be distinguished (see also Ferland et al. [16]:

Elementary method: One of the permeability calculation algorithms is applied to the data of each pair of subsequent time steps and allows calculation of the permeability values based on the differences between the data sets at both time steps (esp. flow front progression).

Hence, for each pair of subsequent time steps permeability values are obtained and these can then be averaged to receive the final measurement values (K_1 and K_2) of the test.

Reference time step method: As with the elementary method permeability values are calculated at each time step, using one of the permeability calculation algorithms. Yet, not the difference to the previous time steps is considered, but always the difference to the very first time step (or another specific time step).

Single step method: Using one of the permeability calculation algorithms, the permeability is calculated with the data obtained at two particular time steps (e.g. the first and the last).

Global method: One of the permeability calculation algorithms is applied to the data of all time steps at once using a fitting procedure.

As listed in Table 4, 15 out of 20 stated the usage of global, two of elementary, two of reference time step and one of single step method.

In summary, it is to be expected that significant variations origin from different methods for data analysis. In order to estimate the magnitude of these variations it was decided to recalculate some of the results using a unified analysis approach. For this, the data sets (fluid injection pressure, dynamic fluid viscosity, flow front data) originally used in step (2) and (3) were collected and evaluated according to a uniform procedure: For step (2), the elliptic paraboloid fitting method introduced by Fauster et al. [9] was applied to all of the collected data sets, and for step (3), the Adams/Rebenfeld algorithm was used. As the paraboloid method allows for the fitting of an elliptic paraboloid to the entire set of flow front data acquired during the radial flow experiments in a single step, it is a global method. Step (2) and (3) were performed at Montanuniversität Leoben for all collected data sets in order to minimise any influence related to data processing. This study was an additional offer to the participants, after the measurement phase of the benchmark study was concluded. Eight data sets (#2a, #2b, #5, #6, #7, #9, #12, #14) were recalculated this way.

To evaluate the influence of differences in step (2) and (3) on the final results, the in-plane permeability characteristics calculated with the individual approach (K_{1ind}, K_{2ind}, β_{ind}) can be compared with those calculated with the unified approach (K_{1uni}, K_{2uni}, β_{uni}). The relative deviation was calculated for every of the 15 tests for each participant, for both materials, and for K_1, K_2 and β (e.g. $\left|\frac{K_{1ind}-K_{1uni}}{K_{1uni}}\right| \cdot 100\%$). The average deviation and the corresponding standard deviations (minimum/maximum error bar) for each individual participant are shown in Figure 11.

The deviations for the orientation angle of the NCF are significantly higher than those for the WF, which corresponds to the high variation of the orientation angle measurements described above. No clear trend was found for the difference between K_1 and K_2, neither for the NCF, nor for the WF. Also the results of the individual approach are not consistently higher or lower compared to the uniform approach. The average deviation for all the data shown in the diagram is 21% for K_1 and K_2 and 3° for β. This presumably corresponds to the magnitude of variation between the participants which is induced by the analysis. The total average coefficient of variation for K_1 and K_2 between the considered data sets is 39% when the individual approaches are applied and 33% when the uniform approach is applied. Hence, significant potential for further reduction of variation is given.

5. Conclusions

The purpose of the presented benchmark exercise was to evaluate the comparability of in-plane permeability characteristics obtained using different measurement systems based on radial flow experiments, and to identify sources of variation. For this purpose, 19 participants with 20 systems measured the permeability of a non-crimp fabric and a woven fabric.

Averaged over all 12 test cases (highest and lowest in-plane permeability of two textiles at three fiber volume contents each) the coefficient of variation (cv) between the permeability values determined with the different systems was 32% and 44% for NCF and WF respectively. On the other hand, the average cv for an individual systems was 8% and 12% for NCF and WF respectively, so the variation between systems is significantly higher than the uncertainty for a single system. Several causes for this difference were identified, leading to the conclusion that strategies to minimise differences in permeability values obtained using different systems will have to focus on these points:

- Cavity deformation is presumably the largest influence and strongly varies among participants. The results show that the stiffness of the injection tools can be strongly limited by inappropriate design.
- There is no uniform strategy on where to measure injection pressure, which might induce variation.
- Any effort to standardize permeability must take into account the methods to determine viscosity. Uncertainty in determination of the fluid viscosity, fitting of viscosity-temperature curves and temperature measurement can induce variation in the magnitude of several percent.
- Stack-wise measurement of areal weight and calculation of corresponding fiber volume content should be mandatory, to consider areal weight variations.
- Differences in the methods used for data analysis induce significant variation.

As a next step, the participants of the benchmark will derive some basic minimum requirements for permeability measurement systems and procedures (radial flow) from these results. Subsequently, smaller and topic-focused benchmarks will deal with remaining questions, e.g. the influence of injection pressure and the best strategy for injection pressure determination. Together with the first and second international benchmark exercise, the

authors are confident that this will provide sufficient data for definition of guidelines for permeability measurement.

Acknowledgement

It is kindly acknowledged that the textile manufacturing companies Saertex GmbH and Hexcel Corporation supported the benchmark by supplying the materials free of charge.

Literature

[1] Parnas RS, Flynn KM, Dal-Favero ME. A permeability database for composites manufacturing. Polymer composites. 1997;18(5):623-33.

[2] Parnas RS, Howard JG, Luce TL, Advani SG. Permeability characterization. 1. A proposed standard reference fabric for permeability. Polymer Composites. 1995;16(6):429-45.

[3] Lundström TS, Stenberg R, Bergstrom R, Partanen H, Birkeland PA. In-plane permeability measurements: a nordic round-robin study. Composites Part A: Applied Science and Manufacturing. 2000;31(1):29-43.

[4] Fauster E, Berg DC, Abliz D, Grössing H, Meiners D, Ziegmann G, et al. Image processing and data evaluation algorithms for reproducible optical in-plane permeability characterization by radial flow experiments. Journal of composite materials. 2017:0021998318780209.

[5] Grössing H, Becker D, Schledjewski R, Mitschang P, Kaufmann S. An evaluation of the reproducibility of capacitve sensor based in-plane permeability measurements: a benchmarking study. eXPRESS Polymer Letters. 2015;9(2):129-42.

[6] Arbter R, Beraud J, Binetruy C, Bizet L, Bréard J, Comas-Cardona S, et al. Experimental determination of the permeability of textiles: a benchmark exercise. Composites Part A: Applied Science and Manufacturing. 2011;42(9):1157-68.

[7] Alms JB, Correia N, Advani SG, Ruiz E. Experimental procedures to run longitudinal injections to measure unsaturated permeability of LCM reinforcements. Permeability Measurement Standard, Permeability Benchmark II, http://cchp meca polymtl ca/permeabilityBenchmarkII html. 2010.

[8] Vernet N, Ruiz E, Advani S, Alms J, Aubert M, Barburski M, et al. Experimental determination of the permeability of engineering textiles: Benchmark II. Composites Part A: Applied Science and Manufacturing. 2014;61:172-84.

[9] Fauster E, Berg DC, May D, Blößl Y, Schledjewski R. Robust evaluation of flow front data for in-plane permeability characterization by radial flow experiments. Advanced Manufacturing: Polymer & Composites Science. 2018;4(1):24-40.

[10] Berg D, Fauster E, Abliz D, Grössing H, Meiners D, Schledjewski R, et al. Influence of test rig configuration and evaluation algorithms on optical radial-flow permeability measurement: A benchmark exercise. Proc 20th Int Conf on Composite Materials, Copenhagen, Denmark2015.

[11] Kissinger C, Mitschang P, Neitzel M, Roder G, Haberland R. Continuous on-line permeability measurement of textile structures. Bridging the Centuries with Sampe's Materials and Processes Technology, Vol 45, Books 1 and 22000. p. 2089-96.
[12] Aranda S, Berg D, Dickert M, Drechsel M, Ziegmann G. Influence of shear on the permeability tensor and compaction behaviour of a non-crimp fabric. Composites Part B: Engineering. 2014;65:158-63.
[13] Louis BM, Di Fratta C, Danzi M, Zogg M, Ermanni P. Improving time effective and robust techniques for measuring in-plane permeability of fibre preforms for LCM processing. New material characteristics to cover new applications needs: SEICO 11; SAMPE Europe 32nd International Technical Conference & Forum; March 28th-29th, 2011, Paris; proceedings 2011 SAMPE Europe International Conference Paris: Society for the Advancement of Material and Process Engineering; 2011. p. 204-11.
[14] Alhussein H, Umer R, Rao S, Swery E, Bickerton S, Cantwell W. Characterization of 3D woven reinforcements for liquid composite molding processes. Journal of materials science. 2016;51(6):3277-88.
[15] Endruweit A, McGregor P, Long A, Johnson M. Influence of the fabric architecture on the variations in experimentally determined in-plane permeability values. Composites Science and Technology. 2006;66(11-12):1778-92.
[16] Ferland P, Guittard D, Trochu F. Concurrent methods for permeability measurement in resin transfer molding. Polymer composites. 1996;17(1):149-58.
[17] Adams KL, Rebenfeld L. Permeability Characteristics of Multilayer Fiber Reinforcements .1. Experimental-Observations. Polymer Composites. 1991;12(3):179-85.
[18] Chan AW, Hwang ST. Anisotropic in-plane permeability of fabric media. Polymer Engineering & Science. 1991;31(16):1233-9.
[19] Adams KL, Miller B, Rebenfeld L, Hwang ST, Chan AW. Forced Inplane Flow of an Epoxy-Resin in Fibrous Networks. Polymer Engineering and Science. 1986;26/20(20):1434-41.
[20] Adams KL, Rebenfeld L. Permeability Characteristics of Multilayer Fiber Reinforcements .2. Theoretical-Model. Polymer Composites. 1991;12(3):186-90.
[21] Adams KL, Russel WB, Rebenfeld L. Radial Penetration of a Viscous-Liquid into a Planar Anisotropic Porous-Medium. International Journal of Multiphase Flow. 1988;14(2):203-15.
[22] Weitzenböck J, Shenoi R, Wilson P. Radial flow permeability measurement. Part A: Theory. Composites Part A: Applied Science and Manufacturing. 1999;30(6):781-96.
[23] Weitzenböck J, Shenoi R, Wilson P. Radial flow permeability measurement. Part B: Application. Composites Part A: Applied Science and Manufacturing. 1999;30(6):797-813.
[24] Pucci MF, Liotier P-J, Drapier S. Tensiometric method to reliably assess wetting properties of single fibers with resins: Validation on cellulosic reinforcements for composites. Colloids and Surfaces A: Physicochemical and Engineering Aspects. 2017;512:26-33.
[25] Pucci MF, Liotier P-J, Drapier S. Capillary wicking in a fibrous reinforcement–Orthotropic issues to determine the capillary pressure components. Composites Part A: Applied Science and Manufacturing. 2015;77:133-41.
[26] Fauster E, Grössing H, Schledjewski R, Materials ESoC. Comparison of algorithms for 2D anisotropic permeability calculation in terms of uncertainty propagation. European Society of Composite Materials), Proc 16th Eur Conf of Composite Materials, Seville, Spain2014.

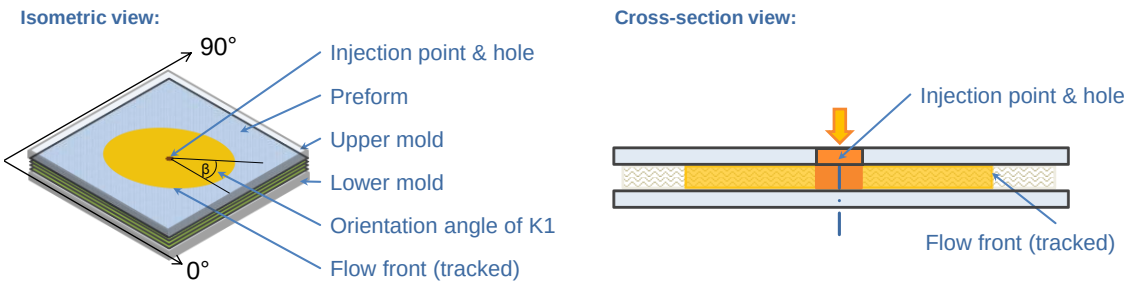

Figure 1: Schematic illustration of the radial injection approach which is the focus of this benchmark exercise.

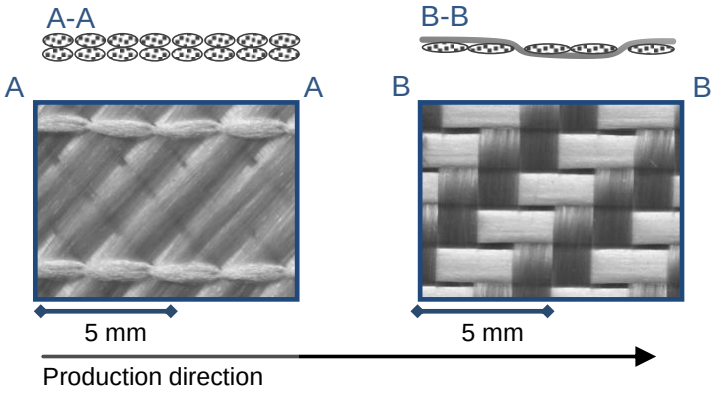

Figure 2: Images of the textiles characterized in this benchmark study.

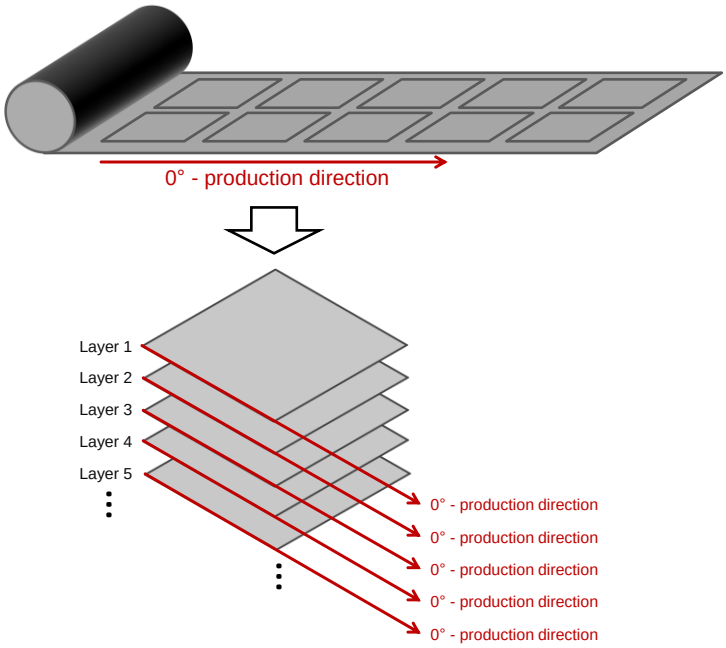

Figure 3: Cutting and stacking of the samples – all layers have identical orientation.

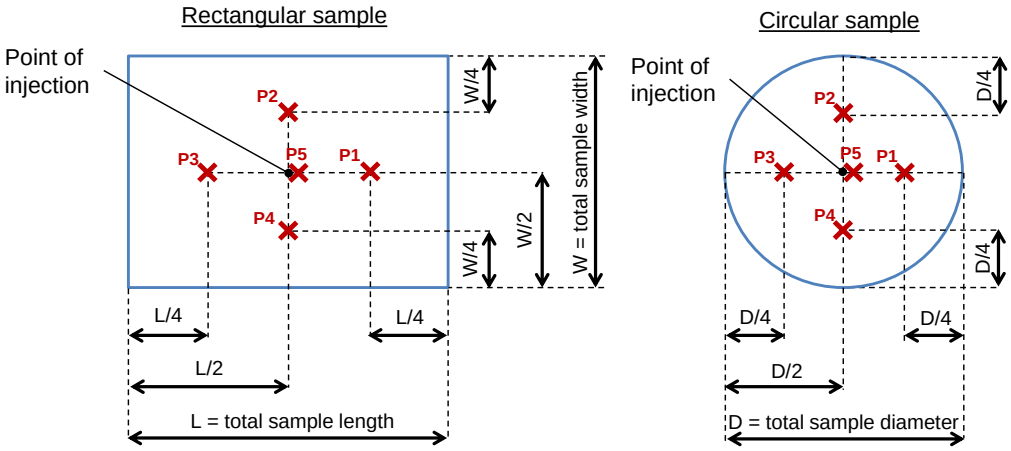

Figure 4: Positions for measurement of the actual cavity height.

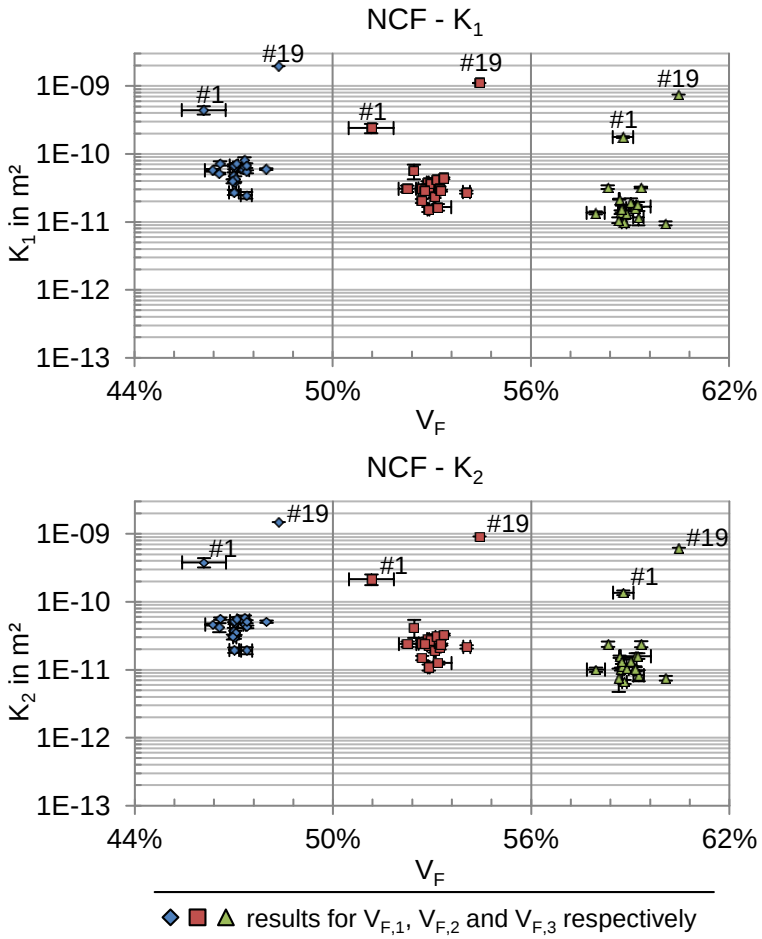

Figure 5: Permeability results for the NCF.

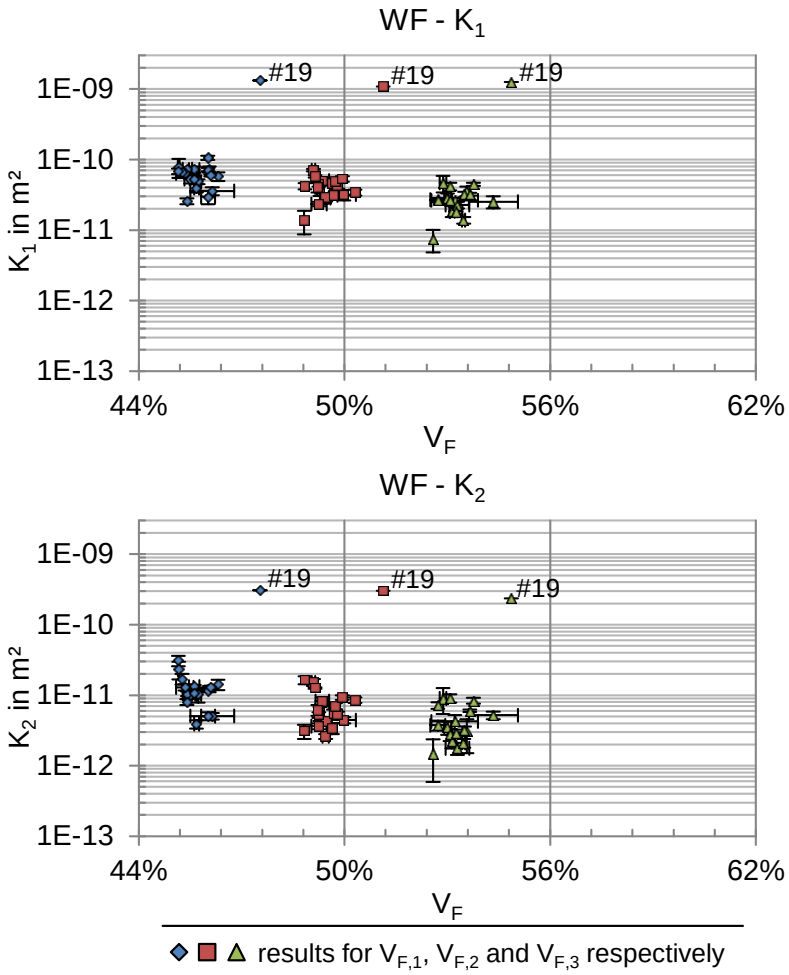

Figure 6: Permeability results for the WF.

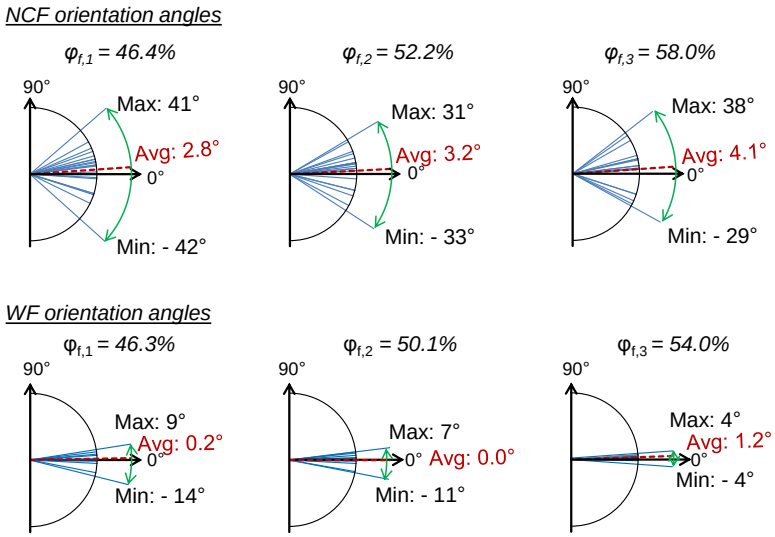

Figure 7: Average orientation angles measured by the participants for the different target fiber volume contents; the dashed line shows the total average over all participants.

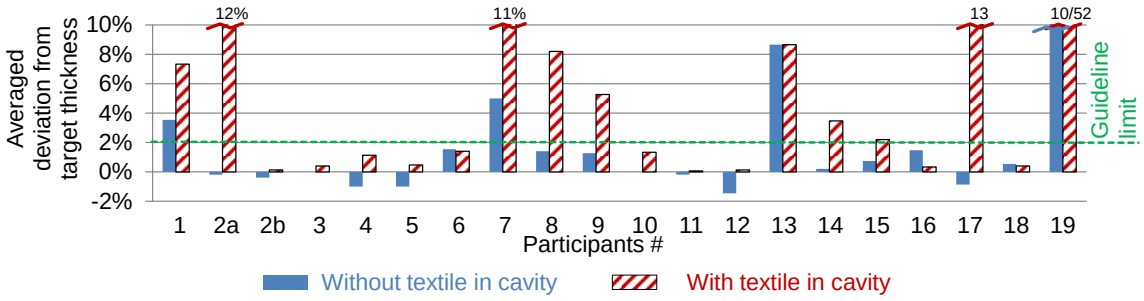

Figure 8: Experimentally determined deviation of the cavity height from the target height.

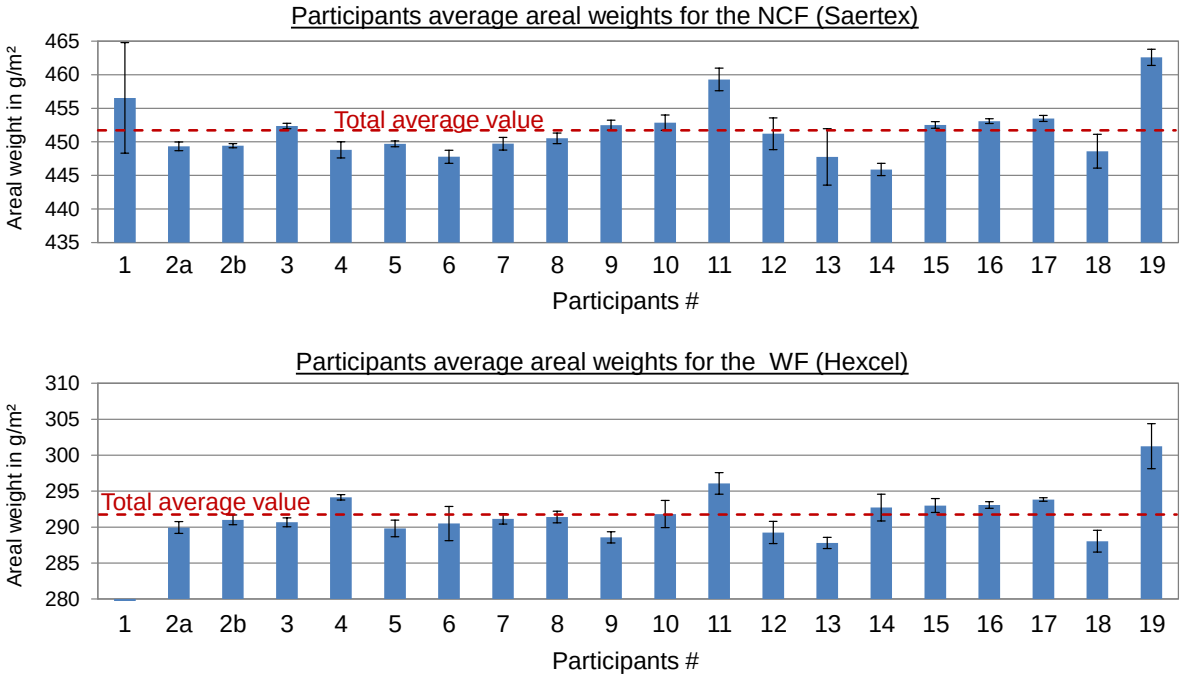

Figure 9: Average areal weights measured for test specimens.

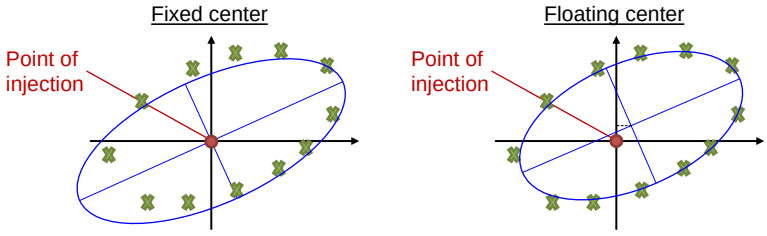

Figure 10: Basic strategies for ellipse modelling – fixed center (left) and floating center (right).

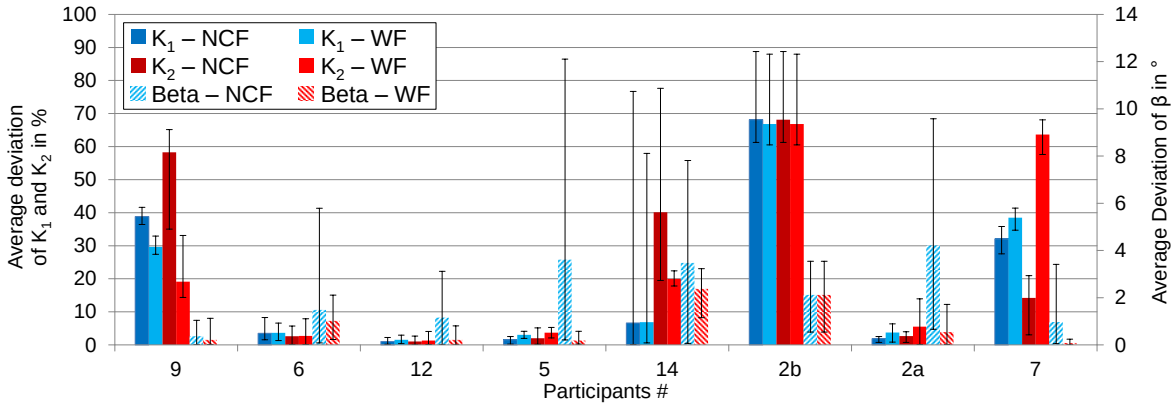

Figure 11: Averaged deviations between results obtained using a unified and individual approach, respectively.

Table 1: List of participants.

Participant	Institution	Department	Country
1	National University of Mar del Plata	Institute of Material Science and Technology	Argentina
2	Montanuniversität Leoben	Processing of Composites Group	Austria
3	Institut de Soudure – Composite Platform		France
4	Ecole Nationale Supérieure des Mines de Douai	Department of Polymers and Composites Technology & Mechanical Engineering	France
5	Institut für Verbundwerkstoffe GmbH	Manufacturing Science	Germany
6	TU Clausthal	Institute of Polymer Materials and Polymer Technology	Germany
7	Technical University Munich	Chair of Carbon Composites	Germany
8	University of Stuttgart	Institute of Aircraft Design	Germany
9	University of Auckland	Faculty of Engineering	New Zealand
10	Institute of Science and Innovation in Mechanical and Industrial Engineering	Composite Materials and Structures Group	Portugal
11	Skoltech	Center for Design, Manufacturing and Materials	Russia
12	ITAINNOVA		Spain
13	ETH Zurich	Department of Mechanical and Process Engineering	Switzerland
14	Koc University	Department of Mechanical Engineering	Turkey
15	Khalifa University	Department of Aerospace Enigneering	UAE
16	National Physical Laboratory	Materials Division	UK
17	Nottingham University	Faculty of Engineering	UK
18	Brigham Young University	Faculty of Manufacturing Engineering Technology	USA
19	Purdue University	Composites Manufacturing & Simulation Center	USA

Table 2: Details of the individual set-ups.

Partici-pant #	Sample size in mm²	Length to width ratio	Tool material (top/bottom)	Flow detection	Monitoring injection pressure[1]	Monitoring temperature[2]	Liter-ature
1	51,129	1:1	glass/metal	optical	none	pressure vessel	
2a[3]	112,687	3:4	glass+steel reinforcement/steel	optical	feed line	feed line	[9,10]
2b[3]	215,812	1:1	aluminum/aluminum	capacitive	prop. valve	tool	[5]
3	95,586	1:1	aluminum/aluminum	pressure (6 sensors)	tool	room	
4	160,000	1:1	metal/PMMA	optical	feed line	room	
5	215,568	1:1	aluminum/aluminum	capacitive	None	tool	[5,11]
6	62,387	1:1	glass+metal reinforcment/metal	optical	feed line	feed line	[10,12]
7	78,287	circular	glass/aluminum	optical	feed line	feed line	
8	89,887	1:1	PMMA/aluminum	optical	feed line	pressure vessel + tool	
9	72,900	1:1	glass/metal	optical	feed line	tool	
10	80,384	circular	metal/metal	pressure (64 sensors)	tool	tool	
11	7,741	circular	PMMA/PMMA	optical	feed line	feed line	
12	107,187	3:4	steel/steel	dielectrical (22 sensors)	feed line	tool	
13	193,487	1:1	metal/metal	pressure	tool	n/a[4]	[13]
14	72,787	1:1	glass-aluminum sandwich/aluminum	optical	feed line	feed line	
15	31,303	circular	metal/glass	optical	feed line	feed line	[14]
16	89,887	1:1	glass+aluminum reinforcement/metal	optical	tool	tool	
17	125,551	circular	aluminium/aluminum	pressure (6 sensors)	tool	pressure vessel	[15]
18	22,387	1:1	PMMA/PMMA	optical	prop. valve	Tool	
19	40,000	1:1	PMMA/PMMA	optical	feed line	pressure vessel	

[1,2]refers to the location of the sensor from which the values are used for calculation

[3]Participant #2 participated in the benchmark with 2 different systems

[4]This was the only system in the benchmark working with constant flow rate instead of constant injection pressure

Table 3: Test plan.

Test series	Material	No. of layers	Fiber volume content (V_F) in %	Injection pressure (gauge) in MPa	No. of repeats	Cavity height in mm
NCF - $V_{F,1}$	NCF	8	46.4	0.1	5	3.00
NCF - $V_{F,2}$		9	52.2	0.2		
NCF - $V_{F,3}$		10	58.0	0.4		
WF - $V_{F,1}$	WF	12	46.3	0.1		
WF - $V_{F,2}$		13	50.1	0.2		
WF - $V_{F,3}$		14	54.0	0.4		

Table 4: Analysis methods implemented by the participants.

Participant #	Algorithm for analysis[1]	Evaluation method[2]	Ellipse-fitting centered[3]	Method of pressure consideration[4]
1	Chan/Hwang	Global Method	yes	average
2a	Adams/Rebenfeld	Global Method	yes	average
2b	Adams/Rebenfeld	Global Method	yes	average
3	n/a	Single Step Method	no	target
4	Chan/Hwang	Global Method	yes	average
5	Adams/Rebenfeld	Global Method	yes	target
6	Modified[5] Chan/Hwang	Global Method	yes	average / single value
7	Adams/Rebenfeld	Elementary Method	yes	average
8	Adams/Rebenfeld	Global Method	no	average
9	Weitzenböck et al.	Reference Time Step Method	yes	single value
10	Adams/Rebenfeld	Global Method	yes	average
11	Chan/Hwang	Global Method	no	average
12	n/a	Global Method	yes	average
13	Chan/Hwang	Elementary Method	yes	single value
14	Weitzenböck et al.	Global Method	yes	average
15	Weitzenböck et al.	Reference Time Step Method	no	average
16	Weitzenböck et al.	Global Method	yes	average
17	Weitzenböck et al.	Elementary Method	yes	average
18	Adams/Rebenfeld	Global Method	yes	average
19	Chan/Hwang	Global Method	yes	target

[1]for detailed explanation we refer to these publications: Chan/Wang: [18]; Adams/Rebenfeld: [17; 19-21]; Weitzenböck et al. [22, 23]
[2]for detailed explanation we refer to Ferland et al. [16]
[3]When fitting an ellipse to the flow data there are two possibilites: Either fix the ellipse-center to the injection point (yes) or to allow the location of the ellipse center to deviate from the injection point (no)
[4]Refers to the way how injection pressure is considered in permeability calculation → Average: All captured values are averaged; single value: for every time step the currently captured pressure value is considered; target: the target injection pressure is assumed
[5]Chan model was modified to correct an error: the inlet radius is stated to be falsely transformed

Table 5: Results for the permeability for the NCF.

Partici-pant #		fiber volume content in % (±cv)	K_1 in 10^{-11} m^2 (±cv)	K_2 in 10^{-11} m^2 (±cv)	Orientation angle of K_1
1	$V_{f,1}$	46.1 (±1.4%)	44.2 (±13.8%)	38.0 (±15.8%)	6.6
	$V_{f,2}$	51.2 (±1.3%)	24.0 (±15.8%)	21.5 (±17.8%)	-33.0
	$V_{f,3}$	58.8 (±0.5%)	17.7 (±3.3%)	13.6 (±7.5%)	-29.0
2a	$V_{f,1}$	47.0 (±0.1%)	6.32(±5.9%)	4.85 (±3.0%)	13.0
	$V_{f,2}$	52.9(±0.1%)	3.77(±4.8%)	2.81(±6.4%)	4.6
	$V_{f,3}$	58.7(±0.2%)	2.16 (±2.0%)	1.56 (±4.2%)	3.9
2b	$V_{f,1}$	47.0 (±0.1%)	4.80 (±11.7%)	3.70 (±11.6%)	-4.97
	$V_{f,2}$	52.9(±0.1%)	3.14(±1.9%)	2.30(±4.0%)	-0.24
	$V_{f,3}$	58.7(±0.0%)	1.39(±5.8%)	1.02(±4.9%)	6.12
3	$V_{f,1}$	47.3(±0.1%)	5.82 (±5.8%)	5.32(±6.1%)	n/a
	$V_{f,2}$	53.2(±0.1%)	3.08(±3.2%)	3.02(±3.6%)	n/a
	$V_{f,3}$	59.2(±0.1%)	1.68(±5.8%)	1.58(±10.4%)	n/a
4[1]	$V_{f,1}$	47.0(±0.2%)	3.79(±3.4%)	2.99(±3.6%)	-3.6
	$V_{f,2}$	52.7(±0.1%)	3.08(±8.0%)	2.43(±9.7%)	-4.1
	$V_{f,3}$	n/a	n/a	n/a	n/a
5	$V_{f,1}$	47.0(±0.1%)	6.78(±4.2%)	5.21(±4.3%)	1.8
	$V_{f,2}$	53.0(±0.1%)	3.62(±5.0%)	2.70(±7.4%)	3.4
	$V_{f,3}$	58.8(±0.1%)	1.59(±8.6%)	1.12 (±9.1%)	4.1
6	$V_{f,1}$	46.4(±0.4%)	5.75(±4.5%)	4.63(±3.5%)	8.5
	$V_{f,2}$	52.3(±0.2%)	3.07(±10.6%)	2.39(±9.3%)	10.1
	$V_{f,3}$	58.0(±0.4%)	1.36(±5.3%)	1.00(±7.6%)	7.4
7a	$V_{f,1}$	47.0(±0.3%)	2.72(±7.9%)	1.95(±9.2%)	11.5
	$V_{f,2}$	52.9(±0.7%)	1.53(±8.6%)	1.09(±10.2%)	7.4
	$V_{f,3}$	58.8(±0.8%)	0.996(±10.4%)	0.663(±6.7%)	13.1
7b	$V_{f,1}$	44.2(±0.3%)	2.72(±7.9%)	1.95(±9.2%)	11.5
	$V_{f,2}$	50.2(±0.7%)	1.53(±8.6%)	1.09(±10.2%)	7.4
	$V_{f,3}$	54.9(±0.8%)	0.996(±10.4%)	0.663(±6.7%)	13.1
8	$V_{f,1}$	47.0(±0.1%)	4.27(±9.1%)	3.50 (±7.2%)	9.6
	$V_{f,2}$	53.1(±0.2%)	2.34(±3.8%)	1.88(±4.7%)	8.7
	$V_{f,3}$	58.9(±0.1%)	1.34(±7.4%)	1.03(±11.0%)	11.8
9	$V_{f,1}$	47.3(±0.2%)	6.55(±7.0%)	4.61(±11.4%)	-26.3
	$V_{f,2}$	53.2(±0.1%)	3.52(±5.4%)	2.46(±10.5%)	-27.6
	$V_{f,3}$	59.1(±0.2%)	1.68(±6.7%)	1.04(±7.9%)	-26.7
10	$V_{f,1}$	47.4(±0.3%)	2.48(±11.6%)	1.92(±12.0%)	29.2
	$V_{f,2}$	53.2(±0.1%)	1.65(±10.9%)	1.26(±5.6%)	20.5
	$V_{f,3}$	59.3(±0.3%)	1.17(±24.0%)	0.832(±18.9%)	29.7
11	$V_{f,1}$	48.0(±0.3%)	5.98(±2.5%)	5.10(±4.2%)	20.0
	$V_{f,2}$	54.0(±0.3%)	2.75(±5.4%)	2.18(±5.3%)	18.5
	$V_{f,3}$	60.1(±0.5%)	0.953(±6.7%)	0.75(±7.9%)	13.0
12	$V_{f,1}$	47.1(±0.5%)	7.24(±7.3%)	5.53(±7.8%)	-17.7
	$V_{f,2}$	53.1(±0.5%)	4.22(±1.7%)	3.11(±7.1%)	-19.4
	$V_{f,3}$	59.0(±0.6%)	1.94(±14.2%)	1.32(±13.2%)	-23.7
13	$V_{f,1}$	46.6(±1.4%)	5.18(±15.3%)	4.20(±14.7%)	22.8
	$V_{f,2}$	52.8(±0.3%)	2.86(±5.6%)	2.41(±7.4%)	10.4

	$V_{f,3}$	58.7(±0.1%)	1.56(±13.2%)	1.32(±7.4%)	4.0
14	$V_{f,1}$	6.6(±0.3%)	7.26(±3.9%)	5.65(±4.0%)	8.1
	$V_{f,2}$	52.5(±0.1%)	5.59(±24.5%)	4.17(±29.5%)	9.3
	$V_{f,3}$	58.3(±0.1%)	3.25(±6.3%)	2.39(±9.3%)	5.1
15	$V_{f,1}$	47.3(±0.1%)	8.11(±7.0%)	5.87(±6.8%)	16.0
	$V_{f,2}$	53.2(±0.1%)	3.08 (±6.2%)	2.10(±5.9%)	13.8
	$V_{f,3}$	59.2(±0.1%)	1.57(±4.3%)	1.02(±6.6%)	16.0
16	$V_{f,1}$	47.4(±0.1%)	5.46(±5.2%)	4.30(±4.7%)	-3.1
	$V_{f,2}$	53.3(±0.1%)	2.89(±3.7%)	2.36(±3.1%)	9.7
	$V_{f,3}$	59.2(±0.1%)	1.81(±8.5%)	1.60(±9.6%)	7.2
17a	$V_{f,1}$	47.4(±0.1%)	6.75(±5.7%)	5.12(±5.2%)	-17.2
	$V_{f,2}$	53.3(±0.1%)	4.39(±3.0%)	3.30(±3.0%)	-14.2
	$V_{f,3}$	59.3(±0.1%)	3.20(±2.7%)	2.40(±10.3%)	-18.2
17b	$V_{f,1}$	46.6(±0.1%)	6.85(±5.7%)	5.20(±5.2%)	-17.2
	$V_{f,2}$	50.2(±0.1%)	4.68(±3.0%)	3.52(±3.0%)	-14.2
	$V_{f,3}$	52.6(±0.1%)	3.73(±2.7%)	2.79(±10.2%)	-18.2
18	$V_{f,1}$	47.0(±0.9%)	3.97(7.8±%)	3.05(±8.9%)	-42.4
	$V_{f,2}$	52.7(±0.3%)	2.04(9.7±%)	1.49(±13.0%)	31.3
	$V_{f,3}$	58.6(±0.3%)	1.06(8.7±%)	0.758(±10.8%)	35.0
19	$V_{f,1}$	48.4(±0.3%)	196(29.0±%)	149(±25.0%)	40.7
	$V_{f,2}$	54.4(±0.2%)	111(11.3±%)	91.7(±9.5%)	29.2
	$V_{f,3}$	60.5(±0.2%)	74.9(12.2±%)	62.2(±20.4%)	38.0

[1]These values have been revised after first results presentation at FPCM14 as a unit conversion error was identified in the analysis software of the participant.

Table 6: Results for the permeability for the WF.

Partici-pant #		fiber volume content in % (±cv)	K_1 in 10^{-11} m^2 (±cv)	K_2 in 10^{-11} m^2 (±cv)	Orientation angle of K_1
1	$V_{f,1}$	n/a	n/a	n/a	n/a
	$V_{f,2}$	n/a	n/a	n/a	n/a
	$V_{f,3}$	n/a	n/a	n/a	n/a
2a	$V_{f,1}$	45.5(±0.2%)	5.28(±13.0%)	0.993(±9.9%)	0.79
	$V_{f,2}$	49.3(±0.1%)	3.87(±21.0%)	0.554(±22.7%)	1.23
	$V_{f,3}$	53.0(±0.1%)	2.86(±15.5%)	0.348(±20.8%)	0.91
2b	$V_{f,1}$	45.7(±0.0%)	4.85(±8.1%)	1.02(±23.1%)	-0.41
	$V_{f,2}$	49.5(±0.1%)	2.83(±2.7%)	0.422(±11.2%)	-0.31
	$V_{f,3}$	53.1(±0.1%)	1.86(±17.8%)	0.223(±21.0%)	0.94
3[1]	$V_{f,1}$	45.6(±0.1%)	7.24(±10.4%)	1.32(±5.7%)	n/a
	$V_{f,2}$	49.4(±0.1%)	5.00(±10.1%)	0.826(±12.7%)	n/a
	$V_{f,3}$	53.2(±0.1%)	2.64(±7.8%)	0.424(±143.3%)	n/a
4[2]	$V_{f,1}$	46.1(±0.1%)	3.59(±10.8%)	0.507(±12.9%)	-0.12
	$V_{f,2}$	50.0(±0.1%)	3.17(±10.1%)	0.444(±16.7%)	-0.67
	$V_{f,3}$	n/a	n/a	n/a	n/a
5	$V_{f,1}$	45.4(±0.1%)	7.26(±4.2%)	1.05(±7.3%)	-0.90
	$V_{f,2}$	49.3(±0.2%)	4.52(±8.8%)	0.524(±8.9%)	0.17
	$V_{f,3}$	53.1(±0.2%)	2.64(±6.6%)	0.279(±19.5%)	14.14
6	$V_{f,1}$	45.3(±0.3%)	6.35(±10.4%)	1.29(±10.3%)	-0.78
	$V_{f,2}$	49.2(±0.2%)	4.03(±15.3%)	0.616(±17.0%)	-1.17
	$V_{f,3}$	52.7(±0.7%)	2.69(±6.2%)	0.374(±16.3%)	-0.01
7a	$V_{f,1}$	45.7(±0.6%)	3.94(±13.6%)	0.389(±13.2%)	0.36
	$V_{f,2}$	49.5(±0.4%)	2.90(±12.2%)	0.260(±7.9%)	-0.12
	$V_{f,3}$	53.3(±0.2%)	2.26(±10.7%)	0.176(±19.6%)	0.77
7b	$V_{f,1}$	43.7(±0.6%)	3.94(±13.6%)	0.389(±13.2%)	0.36
	$V_{f,2}$	46.3(±0.4%)	2.90(±12.2%)	0.260(±7.9%)	-0.12
	$V_{f,3}$	49.8(±0.2%)	2.26(±10.7%)	0.176(±19.6%)	0.77
8	$V_{f,1}$	45.6(±0.0%)	5.36(±7.3%)	1.08(±6.2%)	0.53
	$V_{f,2}$	49.7(±0.1%)	3.10(±7.5%)	0.543(±14.9%)	1.29
	$V_{f,3}$	53.3(±0.0%)	1.83(±8.1%)	0.290(±2.0%)	1.08
9	$V_{f,1}$	45.2(±0.1%)	7.88(±30.5%)	2.32(±28.3%)	-13.68
	$V_{f,2}$	49.1(±0.1%)	7.09(±4.4%)	1.52(±11.1%)	0.25
	$V_{f,3}$	52.9(±0.1%)	4.67(±26.5%)	0.897(±40.0%)	1.92
10	$V_{f,1}$	46.0(±0.1%)	2.97(±21.7%)	0.506(±13.1%)	3.96
	$V_{f,2}$	49.3(±0.3%)	2.33(±7.3%)	0.363(±9.7%)	3.60
	$V_{f,3}$	53.5(±0.2%)	1.38(±10.4%)	0.211(±14.1%)	2.56
11	$V_{f,1}$	46.3(±0.3%)	5.76(±13.7%)	1.41(±16.5%)	5.09
	$V_{f,2}$	50.3(±0.1%)	3.39(±9.6%)	0.852(±9.0%)	1.95
	$V_{f,3}$	54.3(±0.3%)	2.53(±19.3%)	0.520(±12.6%)	3.99
12	$V_{f,1}$	45.3(±0.2%)	6.64(±16.0%)	1.70(±17.2%)	0.99
	$V_{f,2}$	49.1(±0.1%)	5.80(±4.0%)	1.26(±2.4%)	-0.03
	$V_{f,3}$	53.1(±0.3%)	4.16(±12.2%)	0.907(±14.0%)	1.30
13	$V_{f,1}$	45.2(±0.1%)	6.80(±8.9%)	3.11(±16.8%)	4.29
	$V_{f,2}$	48.8(±0.1%)	4.20(±9.8%)	1.64(±13.1%)	0.87

	$V_{f,3}$	52.7(±0.2%)	2.62(±4.9%)	0.714(±10.6%)	0.70
14	$V_{f,1}$	46.0(±0.3%)	10.7(±6.8%)	1.23(±5.8%)	0.96
	$V_{f,2}$	49.6(±0.4%)	4.59(±6.8%)	0.341(±17.8%)	6.59
	$V_{f,3}$	53.6(±0.2%)	3.57(±15.9%)	0.304(±50.2%)	4.38
15	$V_{f,1}$	46.1(±0.1%)	7.24(±10.1%)	1.23(±9.9%)	7.21
	$V_{f,2}$	49.8(±0.1%)	4.29(±10.5%)	0.535(±8.9%)	6.01
	$V_{f,3}$	53.5(±0.2%)	3.21(±8.8%)	0.315(±14.0%)	2.39
16	$V_{f,1}$	46.0(±0.0%)	7.19(±5.4%)	1.16(±2.6%)	-11.45
	$V_{f,2}$	49.7(±0.0%)	4.94(±6.8%)	0.698(±9.9%)	-9.66
	$V_{f,3}$	53.7(±0.1%)	3.24(±4.5%)	0.601(±4.0%)	-1.26
17a	$V_{f,1}$	46.1(±0.0%)	5.94(±3.9%)	1.29(±5.9%)	0.40
	$V_{f,2}$	49.9(±0.0%)	5.32(±9.2%)	0.926(±7.4%)	1.80
	$V_{f,3}$	53.8(±0.0%)	4.45(±5.4%)	0.838(±9.8%)	2.00
17b	$V_{f,1}$	45.9(±0.0%)	5.97(±3.9%)	1.30(±5.9%)	0.40
	$V_{f,2}$	48.3(±0.0%)	5.50(±9.2%)	0.957(±7.4%)	1.80
	$V_{f,3}$	49.9(±0.0%)	4.83(±5.5%)	0.909(±9.8%)	2.00
18	$V_{f,1}$	45.4(±0.2%)	2.57(±13.3%)	0.799(±15.7%)	-2.69
	$V_{f,2}$	48.8(±0.2%)	1.37(±6.7%)	0.311(±10.1%)	-3.45
	$V_{f,3}$	52.6(±0.1%)	0.745(±10.6%)	0.148(±9.9%)	-3.66
19	$V_{f,1}$	47.5(±0.3%)	133(±18.7%)	30.8(±59.4%)	8.52
	$V_{f,2}$	51.1(±0.4%)	108(±25.%)	30.2(±79.4%)	-10.54
	$V_{f,3}$	54.9(±0.7%)	126(±20.6%)	23.6(±17.4%)	0.66

[1] These values have been revised after first results presentation at FPCM14 as a data transfer error was identified by the participant.
[2] These values have been revised after first results presentation at FPCM14 as a unit conversion error was identified in the analysis software of the participant.

Table 7: Coefficients of variation based on all data sets for the in-plane permeability values.

	NCF		**WF**	
	K_1	K_2	K_1	K_2
$V_{f,1}$	27.9%	27.3%	32.0%	50.4%
$V_{f,2}$	30.4%	29.9%	32.6%	56.2%
$V_{f,3}$	38.1%	39.6%	36.5%	55.7%
	32.2%	32.3%	33.7%	54.1%
Average	32.2%		43.9%	
	38.3%			

Table 8: Anisotropy values averaged over data of all participants and corresponding cv.

	NCF		**WF**	
	K_2/K_1	cv	K_2/K_1	cv
$V_{f,1}$	0.78	6%	0.21	37%
$V_{f,2}$	0.78	9%	0.18	39%
$V_{f,3}$	0.75	10%	0.16	31%

Table 9: Normalized non-parallel cavity deformation.

Participant	1	2a	2b	3	4	5	6	7	8	9
ω in %	1.1	2.2	0.5	0.3	1.9	0.4	0.3	0.4	0.7	0.3
Participant	10	11	12	13	14	15	16	17	18	19
ω in %	0.5	0.1	0.3	4.7	0.6	0.7	0.0	1.0	0.6	7.7